The Error Probability of the Fixed-Complexity Sphere Decoder

Joakim Jaldén, *Member, IEEE* , Luis G. Barbero, *Member, IEEE*,
Björn Ottersten, *Fellow, IEEE*, John S. Thompson, *Member, IEEE*

***Abstract*—The fixed-complexity sphere decoder (FSD) has been previously proposed for multiple input-multiple output (MIMO) detection in order to overcome the two main drawbacks of the sphere decoder (SD), namely its variable complexity and its sequential structure. Although the FSD has shown remarkable quasi-maximum likelihood (ML) performance and has resulted in a highly optimized real-time implementation, no analytical study of its performance existed for an arbitrary MIMO system. Herein, the error probability of the FSD is analyzed, proving that it achieves the same diversity as the maximum likelihood detector (MLD) independent of the constellation used. In addition, it can also asymptotically yield ML performance in the high-signal-to-noise ratio (SNR) regime. Those two results, together with its fixed complexity, make the FSD a very promising algorithm for uncoded MIMO detection.**

***Index Terms*—Fixed-complexity sphere decoder (FSD), multiple input-multiple output (MIMO), diversity order, signal detection**

I. Introduction

The use of multiple antennas at both ends of a wireless link, i.e., multiple input-multiple output (MIMO), has become the most relevant technology to improve the capacity and spectral efficiency of wireless communication systems [2]. Concentrating on the receiver end, the design and implementation of efficient detection algorithms is of vital importance to benefit from the additional degrees of freedom available in MIMO systems [3]. This paper presents the error probability analysis of a recently proposed detection algorithm, the fixed-complexity sphere decoder (FSD) [4], that provides good performance at high-SNR and that is optimized for a fully-pipelined real-time hardware implementation [5], [6].

We consider a spatially-multiplexed MIMO system with n_T transmit and n_R receive antennas, denoted as $n_\mathrm{T} \times n_\mathrm{R}$. The vector of received symbols $\mathbf{r} \in \mathbb{C}^{n_\mathrm{R}}$ can be modeled as

$$\mathbf{r} = \mathbf{H}\mathbf{s} + \mathbf{v}\,, \tag{1}$$

where $\mathbf{s} = [s_1 \cdots s_{n_\mathrm{T}}]^\mathrm{T} \in \mathbb{C}^{n_\mathrm{T}}$ denotes the vector of transmitted symbols taken independently from an arbitrary constellation $\mathcal{O}$ of M points with $\mathrm{E}[|s_i|^2] = 1/n_\mathrm{T}$ and where $\mathbf{v} \in \mathbb{C}^{n_\mathrm{R}}$ is the vector of independent complex Gaussian noise samples $v_i \sim \mathcal{CN}(0, \sigma^2)$. The channel matrix $\mathbf{H} \in \mathbb{C}^{n_\mathrm{R} \times n_\mathrm{T}}$ has independent elements $h_{ij} \sim \mathcal{CN}(0,1)$ representing a wireless propagation environment with uncorrelated Rayleigh fading [3]. We assume that the channel is perfectly known at the receiver and that $n_\mathrm{R} \geq n_\mathrm{T}$.

The maximum likelihood detector (MLD) for this scenario is given by

$$\hat{\mathbf{s}}_\mathrm{ML} = \arg \min_{\mathbf{s} \in \mathcal{O}^{n_\mathrm{T}}} \|\mathbf{r} - \mathbf{H}\mathbf{s}\|^2\,. \tag{2}$$

However, the straightforward implementation of the MLD is of exponential $O(M^{n_\mathrm{T}})$ complexity in the number of transmit antennas, making it unfeasible for high-dimensional MIMO systems. Although a more efficient MLD implementation is provided by the sphere decoder (SD) [7], it can also be shown to have an exponential complexity (in the worst case as well as in the average case) of $O(M^{\gamma n_\mathrm{T}})$ with $\gamma \in (0,1]$ [8]. In addition, the SD is a sequential algorithm that has a variable complexity, complicating its real-time hardware implementation [9].

Different alternatives have been proposed to reduce or limit the complexity of the SD while approaching its ML performance. Examples include but are not limited to:

- Combination of the SD with some form of channel matrix ordering to reduce the average complexity of the algorithm [10]. However, the resulting algorithm still suffers from a variable complexity and needs a sequential search.
- Addition of geometric or probabilistic methods to reduce the complexity of the SD as in [11]. In this case, their additional operations and variable complexity make them unsuitable for hardware implementation.

J. Jaldén was with the KTH Signal Processing Lab, School of Electrical Engineering, Royal Institute of Technology, Stockholm, Sweden. He is now with the Institute of Communications and Radio-Frequency Engineering, Vienna University of Technology, Gußhausstr. 25-29 // 389, A-1040 Vienna, Austria. (e-mail: joakim.jalden@nt.tuwien.ac.at).

L. G. Barbero was with the Institute for Digital Communications, Joint Research Institute for Signal & Image Processing, The University of Edinburgh, EH9 3JL Edinburgh, U.K. He is now with the ECIT, Queens University of Belfast, NI Science Park, Queens Road, Queens Island, BT3 9DT Belfast, U.K. (e-mail: l.barbero@ecit.qub.ac.uk).

B. Ottersten is with the ACCESS Linnaeus Center, KTH Signal Processing Lab, Royal Institute of Technology, Osquldas väg 10, S-100 44 Stockholm, Sweden (e-mail: bjorn.ottersten@ee.kth.se). Björn Ottersten is also with securityandtrust.lu, University of Luxembourg

J. S. Thompson is with the Institute for Digital Communications, Joint Research Institute for Signal & Image Processing, The University of Edinburgh, Alexander Graham Bell Building, Kings Buildings, Mayfield Road, EH9 3JL Edinburgh, U.K. (e-mail: john.thompson@ed.ac.uk). John Thompson acknowledges the support of the Scottish Funding Council for the Joint Research Institute with the Heriot-Watt University, which is a part of the Edinburgh Research Partnership.

This research is funded in part by the European Research Council under the European Community's Seventh Framework Programme (FP7/2007-2013) / ERC grant agreement no. 227044. The work was in part presented in [1] at the the International Conference on Acoustics, Speech and Signal Processing in Honolulu, Hawaii, USA, April 2007.

- Use of the K-Best lattice decoder [12] (equivalent to the sequential M-algorithm [13]) to approach quasi-ML performance with fixed complexity. This approach provides a fixed complexity but it is typically higher than the complexity of the SD if quasi-ML performance is to be guaranteed [12].

The FSD is a fixed complexity algorithm that has been proposed in [4] and implemented in real-time on a field-programmable gate array (FPGA) platform in [5], [6] as an alternative to the aforementioned algorithms. Previous numerical studies have also shown quasi-ML performance [4]. In this paper we show that the FSD maintains the diversity order of the MLD with a complexity $O(M^{\sqrt{n_{\mathrm{T}}}})$, which represents an advantage over the exponentially complex sphere decoder (SD). We further analyzse the error probability of the FSD and show that it has a negligible performance degradation compared to that of the MLD in the high-signal-to-noise ratio (SNR) regime. Specifically, it is shown that

$$\lim_{\sigma^2 \to 0} \frac{\mathrm{P}\left(\hat{\mathbf{s}}_{\mathrm{FSD}} \neq \mathbf{s}\right)}{\mathrm{P}\left(\hat{\mathbf{s}}_{\mathrm{ML}} \neq \mathbf{s}\right)} = 1\,, \qquad (3)$$

which indicates that the FSD, in addition to having the same diversity as the MLD, asymptotically achieves ML performance in the high-SNR limit. The diversity and error probability performance achieved by the FSD together with its fixed complexity makes the FSD a very attractive algorithm to solve the detection problem in next-generation MIMO systems.

The structure of the paper is as follows: Section II describes the FSD algorithm and presents simulation results showing its quasi-ML performance. Section III analyzes the error probability of the FSD, taking into account the detection ordering, to give valuable insight into the simulation results presented in Section II. Finally, conclusions are drawn in Section IV.

II. The Fixed-Complexity Sphere Decoder

The description of the FSD is included in this section for completeness. The algorithm has been previously proposed for the detection of uncoded MIMO systems using quadrature amplitude modulation (QAM) constellations [4]. It overcomes the two main drawbacks of the SD from an implementation point of view, i.e., its variable complexity depending on the noise level and the channel conditions and the sequential nature of its tree search phase.

The FSD achieves quasi-ML performance by combining a specific channel matrix ordering with a search over only a fixed number of lattice vectors $\mathbf{Hs}$, generated by a small subset $\mathcal{S} \subset \mathcal{O}^{n_{\mathrm{T}}}$, around the received vector $\mathbf{r}$. The transmitted vector $\mathbf{s} \in \mathcal{S}$ with the smallest Euclidean distance is then selected as the solution. The process can be written as

$$\hat{\mathbf{s}}_{\mathrm{FSD}} = \arg\min_{\mathbf{s} \in \mathcal{S}} \|\mathbf{r} - \mathbf{Hs}\|^2\,. \qquad (4)$$

The FSD, analogously to the SD, can be seen as a constrained tree search through a tree with n_{T} levels where M branches originate from each node [7]. Thus, the solution to (4) can be obtained recursively starting from $i = n_{\mathrm{T}}$ and working backwards until $i = 1$, evaluating all the paths belonging

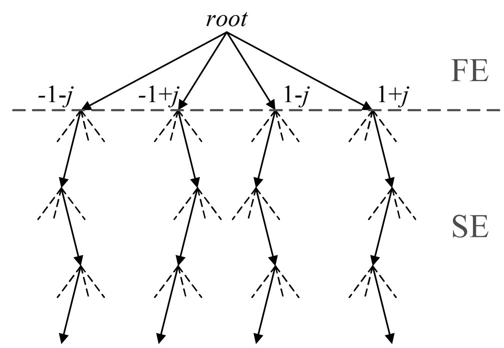

Fig. 1. FE and SE stages in the FSD tree search applied to a 4×4 system with 4-QAM modulation.

to $\mathcal{S}$ [4]. The paths in the tree followed by the FSD are determined by fixing the number of branches per node that are expanded in each level, creating the subset $\mathcal{S}$. In the case of the SD, on the other hand, the number of branches per node expanded in each level is a random variable that depends on the particular level, the search sphere, the channel conditions and the noise level [10] and its average reduces as i decreases (i.e., traversing down the tree) [4].

Although considerable research has been carried out to reduce that average number of branches per node expanded per level by means of a specific channel matrix ordering [10], [14], the resulting algorithms suffer from the same drawbacks as the original SD: variable complexity and a sequential structure. The FSD, on the other hand, takes a completely different approach. It makes use of the channel matrix ordering to fix the number of branches per node while providing a quasi-ML performance. This results in a more optimized hardware implementation of the algorithm compared to that of the SD [5], [6].

A. Generation of the Subset $\mathcal{S}$

The subset searched during the tree phase of the FSD is generated by defining the number of branches per node n_i that are expanded per level for $i = 1, \ldots, n_{\mathrm{T}}$. Thus, the total number of paths followed by the FSD is $\prod_{i=1}^{n_{\mathrm{T}}} n_i$ where $1 \leq n_i \leq M$. In each level, the n_i branches are expanded following the Schnorr-Euchner enumeration [15] so that the first branch corresponds to the decision-feedback equalization (DFE) path.

Although it is difficult to provide a comprehensive analysis of the number of nodes that need to be expanded to achieve quasi-ML performance, the FSD algorithm proposes a general method that can be used for an arbitrary constellation and for any number of antennas [4]. The method consists of having $n_i \in \{1, M\}$ for $i = 1, \ldots, n_{\mathrm{T}}$, and may be described as follows.

- Initially, a full search is performed in the first p levels, expanding all M branches per node, i.e., $n_i = M$ for $i = n_{\mathrm{T}}, \ldots, n_{\mathrm{T}} - p + 1$. This will herein be denoted as the full expansion (FE) stage of the algorithm.
- Secondly, a single search is performed in the remaining $n_{\mathrm{T}} - p$ levels, expanding only one branch per node following the DFE path, i.e., $n_i = 1$ for $i = n_{\mathrm{T}} - p, \ldots, 1$.

This will be denoted as the single expansion (SE) stage of the algorithm.

An example is given in Fig. 1 for the constrained tree search required in a 4×4 system with 4-QAM modulation. Here, the FE stage corresponds to only one level, i.e., $p = 1$. In Section III, we show that this scheme maintains the diversity of the MLD.

The two-stage constrained tree search of the FSD is independent of the noise level and the channel conditions, resulting in a fixed complexity detector as opposed to the variable complexity of the SD. The total number of Euclidean distances calculated in the FSD is M^p, and simulations have shown that quasi-ML performance is achieved with $M^p \ll M^{n_\mathrm{T}}$, i.e., $\mathcal{S}$ is a very small subset of $\mathcal{O}^{n_\mathrm{T}}$, if the two-stage constrained search is combined with a special FSD channel matrix ordering [4].

B. FSD Channel Matrix Ordering

The FSD channel matrix ordering determines the detection ordering of the signals s_i, for $i = 1, \ldots, n_\mathrm{T}$, according to the number of branches per node that are expanded in each level i. The n_T columns of $\mathbf{H}$ are ordered iteratively so that the signals with the *largest* post-processing noise amplification, as defined in [16], are detected in the FE stage. On the other hand, the signals with the smallest post-processing noise amplification are detected in the SE stage.

The steps performed in every iteration are the following, for $i = n_\mathrm{T}, \ldots, 1$:

1) The matrix $\mathbf{Q}_{n_\mathrm{T}-i} = \mathbf{H}^\mathrm{H}_{n_\mathrm{T}-i}\mathbf{H}_{n_\mathrm{T}-i}$ is calculated, where $\mathbf{H}_{n_\mathrm{T}-i}$ is the channel matrix with the $n_\mathrm{T} - i$ columns selected in previous iterations removed. Equivalently, $\mathbf{Q}_{n_\mathrm{T}-i}$ is the principal submatrix of $\mathbf{Q}$, obtained by removing $n_\mathrm{T} - i$ rows and columns from $\mathbf{Q}$.
2) The kth column is selected according to

$$k = \begin{cases} \arg\max_j \, [\mathbf{Q}^{-1}_{n_\mathrm{T}-i}]_{jj} \,, & \text{if } n_i = M \,, \\ \arg\min_j \, [\mathbf{Q}^{-1}_{n_\mathrm{T}-i}]_{jj} \,, & \text{if } n_i = 1 \,, \end{cases} \tag{5}$$

where we assume the correct mapping is done from index j to index k to take into account the columns of $\mathbf{H}$ already removed.

Intuitively, if the maximum number of branches per node is expanded in one level, the *robustness* of the signal is not relevant to the final performance, therefore, the signal that suffers the *largest* post-processing noise amplification can be detected in that level. The opposite occurs when only one branch per node is expanded in a level, the signal with the *smallest* post-processing noise amplification needs to be detected in this level in order not to dramatically worsen the performance.

From a complexity point of view, the FSD ordering of the channel matrix has exactly the same complexity as the vertical-Bell Labs layered space time (V-BLAST) ordering proposed in [16]. Different optimized versions of the latter exist in the literature that could be used for an implementation of the FSD ordering [17].

C. Relation to other Detectors

Naturally, some aspects of the FSD are related to those of other detectors (apart from the obvious relation to SD) and one of the earliest such detectors is the ML-DFE detector, proposed in [18]. It should however be noted that the FSD provides a significant performance improvement over the ML-DFE. The crucial difference between the detectors is that ML-DFE corresponds to a search where only one path in the FE stage is expanded through the SE stage, as opposed to the FSD, where all paths in the FE stage are expanded.

For the specific case of $n_\mathrm{T} = n_\mathrm{R} = 4$ and $p = 1$, the FSD performs the same tree search as the Chase detector with list size M [19], or the parallel detector for V-BLAST systems proposed in [20]. However, the FSD outperforms both algorithms due to a different channel matrix ordering tailored to the two-stage search. The FSD channel matrix ordering in the case of $n_\mathrm{T} = n_\mathrm{R} = 4$ and $p = 1$ corresponds to the ordering independently proposed in [21] and applied to the Chase detector. It should also be noted that detection orderings based on selecting the signals with the *largest* post-processing noise amplification have also been proposed in the context of transmit antenna selection (AS) as a means of maximizing the AS gain of MIMO systems [22], [23].

On a final note we mention that the algorithms in [19] - [21] were proposed as a means of improving the performance of the V-BLAST detector by performing several detections in parallel. On the other hand, the FSD represents a general algorithm proposed in the context of achieving quasi-ML performance in MIMO systems.

D. Performance Example

In this section, a numerical example of the performance of the FSD is given showing the quasi-ML performance achieved in uncoded MIMO detection [4]. The error probability as a function of the SNR has been used as a performance measure, defined as $p_{e\mathrm{FSD}} \triangleq \mathrm{P}\left(\hat{\mathbf{s}}_\mathrm{FSD} \neq \mathbf{s}\right)$ for the FSD and $p_{e\mathrm{ML}} \triangleq \mathrm{P}\left(\hat{\mathbf{s}}_\mathrm{ML} \neq \mathbf{s}\right)$ for the MLD. The SNR is obtained averaging over the channel realizations at one receive antenna and is equal to $\mathrm{SNR} = 1/\sigma^2$.

Fig. 2 shows the error probability of the FSD in a system with $n_\mathrm{T} = n_\mathrm{R} = 4$ system using 4-,16- and 64-QAM modulation. The results have been obtained using 40,000 channel realizations with 300 symbols transmitted in every channel realization. It can be seen how the FSD practically yields ML performance, independent of the noise level and the constellation order. In all cases, the FSD has been simulated with $p = 1$ so that the signal with the *largest* post-processing noise amplification is detected in the FE stage. Remarkably, for the case of 64-QAM, the performance degradation is of only 0.03 dB at SNR = 30 dB while calculating only 64 Euclidean distances, as opposed to the $64^4 = 16,777,216$ Euclidean distances considered in the MLD. A similar example where $n_\mathrm{T} = n_\mathrm{R} = 8$ and $p = 2$ is given in [4, Fig. 5].

Thus, simulations show that the FSD can be used to approach ML performance in MIMO detection with the advantage of having a fixed complexity as opposed to the SD [4].

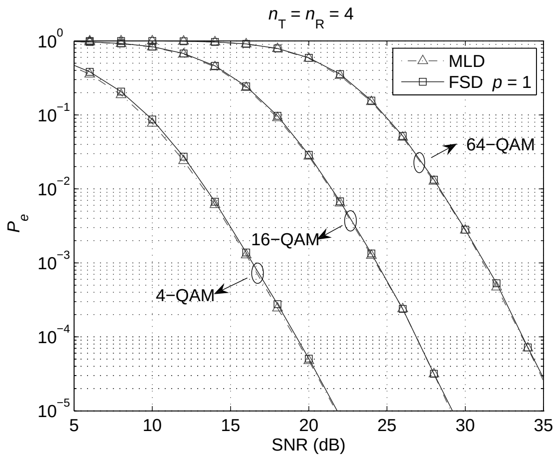

Fig. 2. Error probability of the FSD and the MLD as a function of the SNR in a 4×4 system.

III. Error Probability

The purpose of this Section is to provide an analytical explanation of the results observed in Section II-D and [4], assessing the performance of the algorithm in terms of n_T, n_R and p. In particular, we characterize the high-SNR behavior of the FSD, looking at the diversity order of its error probability. The result shows that the FSD achieves the same diversity as the MLD if the appropriate number of levels p are selected for the FE stage. In addition, the FSD also asymptotically yields ML performance in the high-SNR regime, supporting the quasi-ML performance observed in Section II-D and [4].

A. The FSD Error Probability

When considering the error probability of the FSD it is useful to separate the error event into two mutually exclusive events depending on whether the transmitted vector $\mathbf{s}$ belongs to the set of hypotheses considered by the detector. Specifically,

$$\begin{aligned} p_{e\mathrm{FSD}} &\triangleq \mathrm{P}\left(\hat{\mathbf{s}}_\mathrm{FSD} \neq \mathbf{s}\right) \\ &= \mathrm{P}\left(\hat{\mathbf{s}}_\mathrm{FSD} \neq \mathbf{s} \cap \mathbf{s} \in \mathcal{S}\right) + \mathrm{P}\left(\hat{\mathbf{s}}_\mathrm{FSD} \neq \mathbf{s} \cap \mathbf{s} \notin \mathcal{S}\right) \end{aligned} \quad (6)$$

where $\mathcal{S}$ is given in (4). The first term on the right hand side of (6) asserts that $\mathbf{s}$ belongs to the set of hypotheses considered by the FSD but does not minimize (4). This implies that $\mathbf{s}$ will not minimize (2) and it follows that

$$\mathrm{P}\left(\hat{\mathbf{s}}_\mathrm{FSD} \neq \mathbf{s} \cap \mathbf{s} \in \mathcal{S}\right) \leq \mathrm{P}\left(\hat{\mathbf{s}}_\mathrm{ML} \neq \mathbf{s}\right) . \quad (7)$$

The second term on the right hand side of (6) asserts that the transmitted vector does not belong to the set of hypotheses considered. In this case it is impossible for the FSD to decide in favor of the transmitted message and it follows that

$$\mathrm{P}\left(\hat{\mathbf{s}}_\mathrm{FSD} \neq \mathbf{s} \cap \mathbf{s} \notin \mathcal{S}\right) = \mathrm{P}\left(\mathbf{s} \notin \mathcal{S}\right) . \quad (8)$$

By applying (7) and (8) to (6) it follows that

$$\underbrace{\mathrm{P}\left(\hat{\mathbf{s}}_\mathrm{FSD} \neq \mathbf{s}\right)}_{p_{e\mathrm{FSD}}} \leq \underbrace{\mathrm{P}\left(\hat{\mathbf{s}}_\mathrm{ML} \neq \mathbf{s}\right)}_{p_{e\mathrm{ML}}} + \underbrace{\mathrm{P}\left(\mathbf{s} \notin \mathcal{S}\right)}_{p_{e\mathrm{SE}}} . \quad (9)$$

Thus, if we consider $p_{e\mathrm{ML}}$ and $p_{e\mathrm{SE}}$ to be of different orders of magnitude, the error probability of the FSD can be characterized by the maximum of $p_{e\mathrm{ML}}$ and $p_{e\mathrm{SE}}$. In particular, whenever $p_{e\mathrm{SE}} \ll p_{e\mathrm{ML}}$ the FSD will experience close to optimal performance.

In the high-SNR regime it follows from (9) that the diversity order of the FSD is lower bounded according to

$$d_\mathrm{FSD} \triangleq \lim_{\sigma^2 \to 0} \frac{\log p_{e\mathrm{FSD}}}{\log \sigma^2} \geq \min(d_\mathrm{ML}, d_\mathrm{SE}) , \quad (10)$$

where

$$d_\mathrm{ML} \triangleq \lim_{\sigma^2 \to 0} \frac{\log p_{e\mathrm{ML}}}{\log \sigma^2} = n_\mathrm{R} \quad (11)$$

and

$$d_\mathrm{SE} \triangleq \lim_{\sigma^2 \to 0} \frac{\log p_{e\mathrm{SE}}}{\log \sigma^2} \quad (12)$$

denote the diversity of the MLD and the SE stage respectively. Although (10) initially presents a lower bound, it can be immediately shown that the bound is actually tight by considering the following two cases:

1) $d_\mathrm{SE} \geq d_\mathrm{ML} = n_\mathrm{R}$: the FSD directly achieves the same diversity as the MLD, $d_\mathrm{FSD} = n_\mathrm{R}$, since $p_{e\mathrm{FSD}} \geq p_{e\mathrm{ML}}$.
2) $d_\mathrm{SE} < d_\mathrm{ML}$: in this case, (10) yields $d_\mathrm{FSD} \geq d_\mathrm{SE}$. In addition, (9) indicates that $p_{e\mathrm{FSD}} \geq p_{e\mathrm{SE}}$, i.e., $d_\mathrm{FSD} \leq d_\mathrm{SE}$. Thus, the diversity of the FSD is $d_\mathrm{FSD} = d_\mathrm{SE}$.

Therefore, we can rewrite (10) as

$$d_\mathrm{FSD} = \min(n_\mathrm{R}, d_\mathrm{SE}) \quad (13)$$

which completely characterizes the FSD diversity in terms of d_ML and d_SE.

In addition, it can be seen that in the particular case of $d_\mathrm{SE} > d_\mathrm{ML}$, the bound in (9) yields a performance guarantee that is even stronger than full diversity. Specifically, it follows that also the decoding loss will become negligible at high-SNR. To see this, note that $d_\mathrm{SE} > d_\mathrm{ML}$ implies that the second term in (9) tends to zero at a faster rate than the first term, indicating that the penalty due to sub-optimality will be negligible at high-SNR. The idea, briefly introduced in Section I, is formalized by the following lemma:

Lemma 1: Let d_ML and d_SE be defined according to (11) and (12). If $d_\mathrm{SE} > d_\mathrm{ML}$ it follows that

$$\lim_{\sigma^2 \to 0} \frac{p_{e\mathrm{FSD}}}{p_{e\mathrm{ML}}} = 1 .$$

Proof: Given in Appendix A.

In light of (13) and Lemma 1, it is clear that it is sufficient to compute d_SE in order to complete the analysis of the FSD error probability and to establish under which circumstances the FSD provides quasi-ML performance. Given the structure of the FSD, d_SE would depend on the number of levels p of the SE stage. However, it is not immediately obvious that the assumption on which Lemma 1 relies, i.e., that $d_\mathrm{SE} > d_\mathrm{ML} = n_\mathrm{R}$, can ever be satisfied. In what follows, it is shown that this criterium can be satisfied for even a surprisingly small value of p, provided that the proper detection ordering is applied.

B. The SE Error Event

The second term of (9), $p_{e\mathrm{SE}}$, denotes the probability that the transmitted symbol vector is not included in the set considered by the FSD. This is equivalent to the statement that the transmitted symbol vector does not belong to the set of leaf nodes visited in the tree search [7]. Since every branch is expanded in the FE stage of the tree search, this may be interpreted as the probability that the SE stage excludes the path through the tree corresponding to the transmitted vector.

Let $\mathbf{\Pi}_o$ denote the permutation matrix corresponding to the ordering outlined in Section II-B and let $\mathbf{s}_o \triangleq \mathbf{\Pi}_o^{\mathrm{T}}\mathbf{s}$ denote the correspoding permutation of the transmitted symbol vector. Further, partition $\mathbf{s}_o$ according to

$$\mathbf{s}_o^{\mathrm{T}} = \begin{bmatrix}\mathbf{s}_{o1}^{\mathrm{T}} & \mathbf{s}_{o2}^{\mathrm{T}}\end{bmatrix}$$

where $\mathbf{s}_{o2} \in \mathcal{O}^p$ and $\mathbf{s}_{o1} \in \mathcal{O}^{n_{\mathrm{T}}-p}$ corresponds to the symbols detected in the FE and the SE stage, respectively. Similarly, partition $\mathbf{H}_o \triangleq \mathbf{H}\mathbf{\Pi}_o$ according to

$$\mathbf{H}_o = \begin{bmatrix}\mathbf{H}_{o1} & \mathbf{H}_{o2}\end{bmatrix}$$

where $\mathbf{H}_{o1} \in \mathbb{C}^{n_{\mathrm{R}}\times n_{\mathrm{T}}-p}$ and $\mathbf{H}_{o2} \in \mathbb{C}^{n_{\mathrm{R}}\times p}$. As the SE branch expanding from $\mathbf{s}_{o2}$ corresponds to the DFE estimate of $\mathbf{s}_{o1}$ (given $\mathbf{s}_{o2}$) it follows that

$$p_{e\mathrm{SE}} \triangleq \mathrm{P}\left(\mathbf{s} \notin \mathcal{S}\right) = \mathrm{P}\left(\hat{\mathbf{s}}_{o1} \neq \mathbf{s}_{o1}\right) .$$

In the above, $\hat{\mathbf{s}}_{o1}$ denotes the DFE estimate of $\mathbf{s}_{o1}$ obtained based on the data model

$$\tilde{\mathbf{r}} = \mathbf{H}_{o1}\mathbf{s}_{o1} + \mathbf{v} \tag{14}$$

where $\tilde{\mathbf{r}} \triangleq \mathbf{r} - \mathbf{H}_{o2}\mathbf{s}_{o2}$, as the contribution of $\mathbf{s}_{o2}$ in $\mathbf{r}$ has been perfectly cancelled.

A first observation based on (14) is that the error probability of the FSD does not depend on the internal ordering of columns within $\mathbf{H}_{o2}$. The error probability does, however, depend on the overall ordering, o, through the subset of columns selected for $\mathbf{H}_{o1}$ as well as the internal ordering of these columns. A similar situation is encountered in the analysis of antenna selection methods for spatial multiplexing systems with linear receivers [24]. In this context, the transmitter selects a subset of the available antennas (columns of $\mathbf{H}$) based on the realization of $\mathbf{H}$ and spatially multiplexed independent data streams across the selected antennas. At the receiver, a linear zero forcing (ZF) or minimum mean-square error (MMSE) detector is used to separate the streams. In fact, determining $\mathrm{P}\left(\hat{\mathbf{s}}_{o1} \neq \mathbf{s}_{o1}\right)$ is equivalent to determining the error probability of such a system transmitting from $l = n_{\mathrm{T}} - p$ antennas.

In the context of antenna selection it has been conjectured that the maximum diversity order of such a system is [23]

$$\begin{aligned} d_{\mathrm{AS}} &\triangleq (n_{\mathrm{R}} - l + 1)(n_{\mathrm{T}} - l + 1) \\ &= (n_{\mathrm{R}} - n_{\mathrm{T}})(p+1) + (p+1)^2 . \end{aligned}$$

This conjecture was also recently proven under the assumption of a ZF or a ZF-DFE receiver [25], the latter being equivalent to the SE stage of the FSD. Specifically, for the FSD it follows from [23], [25] that

$$d_{\mathrm{SE}} \leq d_{\mathrm{SE,opt}} \triangleq (n_{\mathrm{R}} - n_{\mathrm{T}})(p+1) + (p+1)^2 , \tag{15}$$

regardless of the detection ordering, $o = o(\mathbf{H})$, used.

Naturally, the optimal ordering (in the sense that it minimizes $p_{e\mathrm{SE}}$ over all orderings) may be obtained by a brute force search. However, this would clearly be impractical from an implementation point of view. Thus, it is reassuring to know that there are efficiently computable orderings which are *diversity optimal* in the sense that they obtain the maximal FSD diversity order and satisfy (15) with equality. For instance, the fast antenna subset selection strategy of [23], [26] could be used to implement such a detection ordering. The proof of optimality is given in [23]. This said, it should also be noted that diversity optimality is a nontrivial property and that for instance a fixed ordering (independent of $\mathbf{H}$) would only achieve a diversity order of

$$d_{\mathrm{SE,fixed}} \triangleq (n_{\mathrm{R}} - n_{\mathrm{T}} + p + 1)$$

for $0 \leq p \leq n_{\mathrm{T}} - 1$. To see this, note that this scenario is equivalent to the standard ZF-DFE scenario [3], with n_{R} receive- and $l = n_{\mathrm{T}} - p$ transmit-antennas. In the optimal ordering scenario, it is illustrative to note that, in the special case of $n_{\mathrm{R}} = n_{\mathrm{T}}$, the FSD achieves full diversity if the necessary and sufficient condition

$$d_{\mathrm{SE}} = (p+1)^2 \geq n_{\mathrm{R}}$$

is satisfied, which implies

$$p \geq \sqrt{n_{\mathrm{T}}} - 1 .$$

This clearly represents a difference compared to the fixed ordering scenario, where $p \geq n_{\mathrm{T}} - 1$ is required to achieve full diversity. In addition, the concept of a diversity optimal ordering stands in sharp contrast to the results of the standard DFE (V-BLAST) detector, in which case a channel dependent detection ordering cannot improve the diversity order [25], [27].

Naturally, we are particularly interested in the ordering originally proposed for the FSD in [4] (c.f. Section II-B) as this ordering has been previously shown to provide close to optimal performance through simulations and is efficiently computable. Thus, we will complete the FSD analysis by proving the diversity optimality of this ordering.

C. The FSD Detection Ordering

Linear detectors and their decision feedback counterparts are typically analyzed through the concept of post-processing SNR [3], which corresponds to the SNR experienced by each symbol in $\mathbf{s}$ after linear filtering at the input to the threshold detector. For the system model in (14), the (ZF) *minimum post-processing SNR* is defined by

$$\rho_{\min}^{(\mathrm{ZF})} \triangleq \min_j \frac{1}{n_{\mathrm{T}}[(\mathbf{H}_{o1}^{\mathrm{H}}\mathbf{H}_{o1})^{-1}]_{jj}\sigma^2}$$

for $j = 1, \ldots, n_{\mathrm{T}} - p$, and the diversity order of the ZF and the ZF-DFE detectors is lower bounded according to

$$d_{\mathrm{SE}} = \lim_{\sigma^2\to 0} \frac{\log \mathrm{P}\left(\hat{\mathbf{s}}_{o1} \neq \mathbf{s}_{o1}\right)}{\log \sigma^2} \geq \lim_{\sigma^2\to 0} \frac{\log \mathrm{P}(\rho_{\min}^{(\mathrm{ZF})} \leq 1)}{\log \sigma^2} ,$$

see, e.g., [23]. Furthermore, noting that $\rho_{\min}^{(\mathrm{ZF})}$ can be lower bounded as

$$\rho_{\min}^{(\mathrm{ZF})} \geq \frac{\lambda_1(\mathbf{H}_{o1}^{\mathrm{H}}\mathbf{H}_{o1})}{n_{\mathrm{T}}\sigma^2},$$

where $\lambda_1(\mathbf{H}_{o1}^{\mathrm{H}}\mathbf{H}_{o1})$ denotes the smallest eigenvalue[1] of $\mathbf{H}_{o1}^{\mathrm{H}}\mathbf{H}_{o1}$ [24], it follows that

$$d_{\mathrm{SE}} \geq \lim_{x\to 0}\frac{\log \mathrm{P}\left(\lambda_1(\mathbf{H}_{o1}^{\mathrm{H}}\mathbf{H}_{o1}) \leq x\right)}{\log x}. \tag{16}$$

Thus, the bound in (16) quantifies the notion that the error probability of the ZF detector is characterized by the minimum eigenvalue of the channel matrix. In particular, computing the limit on the right hand side of (16) for the FSD detection ordering and combining the result with that of (15) yields a (tight) bound on the FSD diversity order.

Although closed form expressions for the distribution of the eigenvalues of $\mathbf{H}_{o1}^{\mathrm{H}}\mathbf{H}_{o1}$ are difficult to obtain, it is possible to bound these eigenvalues in terms of the eigenvalues of the Gram matrix of the full channel matrix, $\mathbf{H}^{\mathrm{H}}\mathbf{H}$. To this end, we consider the following key results:

Lemma 2: Let $\mathbf{A} \in \mathbb{C}^{n\times n}$ be a positive semi-definite (PSD) matrix. Further, let q be given by

$$q = \arg\max_j [\mathbf{A}^{-1}]_{jj}. \tag{17}$$

and let $\mathbf{A}_1$ be the principal submatrix obtained by deleting the qth row and column of $\mathbf{A}$[2]. Then

$$\lambda_i(\mathbf{A}_1) \geq \frac{1}{n}\lambda_{i+1}(\mathbf{A}), \quad i = 1,\ldots,n-1. \tag{18}$$

Proof: Given in Appendix B.

Corollary 3: Given the FSD detection ordering outlined in Section II-B, the smallest eigenvalue of $\mathbf{H}_{o1}^{\mathrm{H}}\mathbf{H}_{o1}$ satisfies

$$\lambda_{p+1}(\mathbf{H}^{\mathrm{H}}\mathbf{H}) \geq \lambda_1(\mathbf{H}_{o1}^{\mathrm{H}}\mathbf{H}_{o1}) \geq \kappa\lambda_{p+1}(\mathbf{H}^{\mathrm{H}}\mathbf{H}) \tag{19}$$

where

$$\kappa \triangleq \frac{(n_{\mathrm{T}}-p)!}{n_{\mathrm{T}}!} > 0$$

Proof: Let $\mathbf{Q} \triangleq \mathbf{H}^{\mathrm{H}}\mathbf{H} \in \mathbb{C}^{n_{\mathrm{T}}\times n_{\mathrm{T}}}$ and let $\mathbf{Q}_p$ be a principal submatrix obtained by sucessively removing p columns and rows from $\mathbf{Q}$ accoring to the criterion in (17). By repeated application of Lemma 2 it follows that

$$\begin{aligned}\lambda_1(\mathbf{Q}_p) \geq &\frac{1}{(n_{\mathrm{T}}-p+1)}\lambda_2(\mathbf{Q}_{p-1})\\ \geq &\frac{1}{(n_{\mathrm{T}}-p+1)(n_{\mathrm{T}}-p+2)}\lambda_3(\mathbf{Q}_{p-2})\\ &\vdots\\ \geq &\frac{1}{(n_{\mathrm{T}}-p+1)\cdots(n_{\mathrm{T}}-0)}\lambda_{p+1}(\mathbf{Q}_0)\\ = &\kappa\lambda_{p+1}(\mathbf{Q})\end{aligned}$$

where $\mathbf{Q}_0 \triangleq \mathbf{Q}$ by definition. Since $\mathbf{H}_{o1}^{\mathrm{T}}\mathbf{H}_{o1}$ equals $\mathbf{Q}_p$ up to a permutation of the rows and columns it holds that $\lambda_1(\mathbf{H}_{o1}^{\mathrm{H}}\mathbf{H}_{o1}) = \lambda_1(\mathbf{Q}_p)$ and the lower bound on $\lambda_1(\mathbf{H}_{o1}^{\mathrm{H}}\mathbf{H}_{o1})$ follows. The upper bound follows directly from the interlacing property of eigenvalues of principal submatrices [28]. ∎

The interpretation of the corollary is that the minimum eigenvalue of $\mathbf{H}_{o1}^{\mathrm{H}}\mathbf{H}_{o1}$ behaves similarly to $\lambda_{p+1}(\mathbf{H}^{\mathrm{H}}\mathbf{H})$. In particular, it follows directly that

$$\begin{aligned}&\lim_{x\to 0}\frac{\log \mathrm{P}\left(\lambda_1(\mathbf{H}_{o1}^{\mathrm{H}}\mathbf{H}_{o1}) \leq x\right)}{\log x}\\ &= \lim_{x\to 0}\frac{\log \mathrm{P}\left(\lambda_{p+1}(\mathbf{H}^{\mathrm{H}}\mathbf{H}) \leq x\right)}{\log x}\\ &= (n_{\mathrm{R}}-n_{\mathrm{T}})(p+1) + (p+1)^2,\end{aligned} \tag{20}$$

where the last equality follows by [29, Th. 1] or as a special case of [30, Th. 4]. Combining (20) with (16), yields a lower bound on d_{SE} that coincides with the upper bound in (15). It follows directly that

$$d_{\mathrm{SE}} = (n_{\mathrm{R}}-n_{\mathrm{T}})(p+1) + (p+1)^2. \tag{21}$$

Finally, inserting (21) into (13) yields the diversity order of the FSD. We formalize this in the following theorem, which is the main contribution of this paper:

Theorem 4: The FSD diversity order is given by

$$d_{\mathrm{FSD}} = \min(\, n_{\mathrm{R}}\,,\, (n_{\mathrm{R}}-n_{\mathrm{T}})(p+1) + (p+1)^2\,). \tag{22}$$

It is important to note that this diversity result has been obtained by looking only at the ordering that takes place in the FE stage, represented by (17). Thus, selecting the signals with the *largest* post-processing noise amplification in the FE stage is a sufficient condition to achieve (21). Furthermore, by ordering the signals to be detected in the SE stage according to the FSD ordering, an additional coding gain can be achieved but no further diversity gain [31].

Different relevant conclusions regarding the performance of the FSD can be drawn from (22). Firstly, for an arbitrary MIMO system following (1), the FSD has the same diversity as the MLD provided $(n_{\mathrm{R}}-n_{\mathrm{T}})(p+1)+(p+1)^2 \geq n_{\mathrm{R}}$. Furthermore, the FSD asymptotically provides ML performance in the high-SNR regime if $(n_{\mathrm{R}}-n_{\mathrm{T}})(p+1)+(p+1)^2 > n_{\mathrm{R}}$, as indicated by Lemma 1. In particular, if we consider the numerical results of Section II-D and [4], the following can now be stated:

1) In a 4×4 system, the FSD with $p=1$ provides the same diversity as the MLD since $p = \sqrt{n_{\mathrm{T}}}-1$. However, it can be seen in Fig. 2 how the (de)coding loss is negligible, effectively yielding quasi-ML performance.
2) In an 8×8 system, the FSD with $p=2$ provides asymptotical ML performance since $p > \sqrt{n_{\mathrm{T}}}-1$.

It should be noted that those results are completely independent of the constellation $\mathcal{O}$ used, further indicating the relevance of the FSD as a MIMO detection algorithm.

Finally, although the study presented here has concentrated on the assumption of uncorrelated Rayleigh fading due to its mathematical tractability, it follows by [32] that the results hold true also for a large class of fading distributions, including correlated Ricean channels.

[1] In the rest of the paper, $\lambda_1(\mathbf{Q}) \leq \ldots \leq \lambda_n(\mathbf{Q})$ denote the ordered eigenvalues of an $n\times n$ matrix $\mathbf{Q}$.

[2] It should be noted that (17) corresponds to one iteration of the FSD ordering for the FE stage, as shown by (5).

IV. Conclusion

This paper presents an error probability analysis of the recently proposed FSD algorithm in the context of MIMO detection. The FSD algorithm combines a fixed complexity search over the tree representation of a spatially multiplexed MIMO system with a specific detection ordering. It has been previously shown to provide quasi-ML performance and results in a highly optimized hardware implementation compared to the original SD, especially for large number of antennas and constellation orders. However, no analytic proof of its performance was available.

By studying the FE and SE stages in the FSD and its detection ordering, this paper proves that the FSD can provide the same diversity order as the MLD. In addition, depending on the number of levels considered in the FE stage, the FSD can also yield asymptotically ML performance in the high-SNR regime. In particular, it has been shown that, by selecting the signals with the *largest* post-processing noise amplification in the FE stage of the algorithm, the diversity of the SE stage grows beyond the diversity order of the MLD. This result has been linked to the concept of transmit antenna selection, where a subset of the transmit antennas are selected to send data streams over the wireless channel. In essence, by fully enumerating p (carefully selected) layers in the tree search, it is possible to remove the influence of the p weakest eigenmodes on the subsequent ZF-DFE step. In addition, an expression has been obtained to establish the number of levels that need to be considered in the FE stage in an arbitrary MIMO system if full diversity or asymptotic ML performance is to be achieved.

Appendix A
Proof of Lemma 1

Since $d_{\mathrm{SE}} > d_{\mathrm{ML}}$ there exists $\delta > 0$ such that $d_{\mathrm{SE}} - d_{\mathrm{ML}} - 2\delta > 0$. For sufficiently small σ^2 it follows by (11) and (12) that

$$\frac{\log p_{e\mathrm{ML}}}{\log \sigma^2} \leq d_{\mathrm{ML}} + \delta \Leftrightarrow p_{e\mathrm{ML}} \geq (\sigma^2)^{d_{\mathrm{ML}}+\delta}$$

and

$$\frac{\log p_{e\mathrm{SE}}}{\log \sigma^2} \geq d_{\mathrm{SE}} - \delta \Leftrightarrow p_{e\mathrm{SE}} \leq (\sigma^2)^{d_{\mathrm{SE}}-\delta} .$$

It follows that

$$\frac{p_{e\mathrm{SE}}}{p_{e\mathrm{ML}}} \leq \frac{(\sigma^2)^{d_{\mathrm{SE}}-\delta}}{(\sigma^2)^{d_{\mathrm{ML}}+\delta}} = (\sigma^2)^{d_{\mathrm{SE}}-d_{\mathrm{ML}}-2\delta}$$

for sufficiently small σ^2, which implies that

$$\limsup_{\sigma^2 \to 0} \frac{p_{e\mathrm{SE}}}{p_{e\mathrm{ML}}} = 0$$

since $d_{\mathrm{SE}} - d_{\mathrm{ML}} - 2\delta > 0$. By (9) it follows that

$$\frac{p_{e\mathrm{FSD}}}{p_{e\mathrm{ML}}} \leq \frac{p_{e\mathrm{ML}}}{p_{e\mathrm{ML}}} + \frac{p_{e\mathrm{SE}}}{p_{e\mathrm{ML}}}$$

and

$$\limsup_{\sigma^2 \to 0} \frac{p_{e\mathrm{FSD}}}{p_{e\mathrm{ML}}} \leq 1 .$$

However, as

$$\frac{p_{e\mathrm{FSD}}}{p_{e\mathrm{ML}}} \geq 1$$

for any $\sigma^2 \geq 0$ (due to the optimality of MLD) the assertion of the lemma follows. ■

Appendix B
Proof of Lemma 2

Note first that it can be assumed, without loss of generality, that $\mathbf{A}$ is such that $q = 1$. This follows since the statement of Lemma 2 is invariant to permutations of the rows and columns of $\mathbf{A}$. Let the eigenvalue decomposition of $\mathbf{A}$ be given by

$$\mathbf{A} = \sum_{i=1}^{n} \eta_i \mathbf{u}_i \mathbf{u}_i^{\mathrm{H}} \tag{23}$$

where (for notational simplicity) $\eta_i \triangleq \lambda_i(\mathbf{A}) \geq 0$ for $i = 1, \ldots, n$ denotes the ith eigenvalue of $\mathbf{A}$, such that $\eta_1 \leq \ldots \leq \eta_n$, and $\mathbf{u}_i$ are the corresponding eigenvectors. By partitioning the eigenvectors of $\mathbf{A}$ according to

$$\mathbf{u}_i = \begin{bmatrix} v_i \\ \mathbf{w}_i \end{bmatrix} \tag{24}$$

where $v_i \in \mathbb{C}$ and $\mathbf{w}_i \in \mathbb{C}^{n-1}$ the inverse of $\mathbf{A}$ can be obtained as

$$\begin{aligned} \mathbf{A}^{-1} &= \sum_{i=1}^{n} \eta_1^{-1} \mathbf{u}_i \mathbf{u}_i^{\mathrm{H}} \\ &= \sum_{i=1}^{n} \eta_i^{-1} \begin{bmatrix} v_i \\ \mathbf{w}_i \end{bmatrix} \begin{bmatrix} v_i^{\mathrm{H}} & \mathbf{w}_i^{\mathrm{H}} \end{bmatrix} \\ &= \sum_{i=1}^{n} \eta_i^{-1} \begin{bmatrix} |v_i|^2 & v_i \mathbf{w}_i^{\mathrm{H}} \\ \mathbf{w}_i v_i^{\mathrm{H}} & \mathbf{w}_i \mathbf{w}_i^{\mathrm{H}} \end{bmatrix} . \end{aligned} \tag{25}$$

Note that the first (and maximal) diagonal element of $\mathbf{A}^{-1}$ is given by

$$[\mathbf{A}^{-1}]_{11} = \sum_{i=1}^{n} \eta_i^{-1} |v_i|^2. \tag{26}$$

For the remaining diagonal elements it follows that

$$\begin{aligned} \max_{i=2,\ldots,n} [\mathbf{A}^{-1}]_{ii} &\overset{(a)}{\geq} \frac{1}{(n-1)} \sum_{j=2}^{n} [\mathbf{A}^{-1}]_{jj} \\ &\overset{(b)}{=} \frac{1}{(n-1)} \sum_{i=1}^{n} \eta_i^{-1} \sum_{j=1}^{n-1} [\mathbf{w}_i \mathbf{w}_i^{\mathrm{H}}]_{jj} \\ &= \frac{1}{(n-1)} \sum_{i=1}^{n} \eta_i^{-1} \|\mathbf{w}_i\|^2 \\ &\overset{(c)}{=} \frac{1}{(n-1)} \sum_{i=1}^{n} \eta_i^{-1} (1 - |v_i|^2) \end{aligned} \tag{27}$$

where (a) follows since the maximum diagonal value must be larger than or equal to the average; (b) follows from the expansion in (25); and (c) is due to $|v_i|^2 + \|\mathbf{w}_i\|^2 = \|\mathbf{u}_i\|^2 = 1$.

The assumption that the maximal diagonal value of $\mathbf{A}^{-1}$ is given by $[\mathbf{A}^{-1}]_{11}$ (i.e., $q = 1$) is equivalent to

$$[\mathbf{A}^{-1}]_{11} \geq \max_{i=2,\ldots,n} [\mathbf{A}^{-1}]_{ii} , \tag{28}$$

which through (26) and (27) yields

$$\sum_{i=1}^{n} \eta_i^{-1} |v_i|^2 \geq \frac{1}{(n-1)} \sum_{i=1}^{n} \eta_i^{-1} (1 - |v_i|^2) .$$

or equivalently

$$\begin{aligned}&\sum_{i=1}^{n}\eta_i^{-1}[(n-1)|v_i|^2-(1-|v_i|^2)]\\&=\sum_{i=1}^{n}\eta_i^{-1}(n|v_i|^2-1)\geq 0\,.\end{aligned}\tag{29}$$

Normalizing (29) by dividing by η_1^{-1} yields

$$\begin{aligned}0\leq&\sum_{i=1}^{n}\frac{\eta_1}{\eta_i}(n|v_i|^2-1)\\=&\sum_{i=1}^{k}\frac{n\eta_1}{\eta_i}|v_i|^2+\sum_{i=k+1}^{n}\frac{n\eta_1}{\eta_i}|v_i|^2-\sum_{i=1}^{n}\frac{\eta_1}{\eta_i}\\\leq&\sum_{i=1}^{k}\frac{n\eta_1}{\eta_1}|v_i|^2+\sum_{i=k+1}^{n}\frac{n\eta_1}{\eta_{k+1}}|v_i|^2-\frac{\eta_1}{\eta_1}-\sum_{i=2}^{k+1}\frac{\eta_1}{\eta_i}\\\leq& n\sum_{i=1}^{k}|v_i|^2+\frac{n\eta_1}{\eta_{k+1}}\sum_{i=k+1}^{n}|v_i|^2-\frac{\eta_1}{\eta_1}-\sum_{i=2}^{k+1}\frac{\eta_1}{\eta_i}\end{aligned}\tag{30}$$

By introducing τ, defined according to

$$\tau\triangleq\sum_{i=1}^{k}|v_i|^2\,,\tag{31}$$

and noting that

$$\sum_{i=k+1}^{n}|v_i|^2=1-\tau\tag{32}$$

the last line of (30) yields

$$n\tau+\frac{n\eta_1}{\eta_{k+1}}(1-\tau)-1-\sum_{i=2}^{k}\frac{\eta_1}{\eta_i}-\frac{\eta_1}{\eta_{k+1}}\geq 0\,.\tag{33}$$

Further, let α be defined according to

$$\alpha\triangleq\frac{\eta_1}{\eta_{k+1}}\,.\tag{34}$$

By the interlacing property for eigenvalues of principal submatrices [28] it follows that

$$\eta_k\leq\lambda_k(\mathbf{A}_1)\leq\eta_{k+1}\,.$$

Thus, whenever $\eta_k\geq n^{-1}\eta_{k+1}$ the assertion in (18) is true for *any* principal submatrix of $\mathbf{A}$, regardless of the selection criterium. Therefore, in order to prove the lemma, we need only to consider the opposite case $\eta_k<n^{-1}\eta_{k+1}$. Note also that this assumption implies that

$$\eta_1=\alpha\eta_{k+1}>\alpha n\eta_k\geq\alpha n\eta_i\,,\quad i=1,\ldots,k\,,\tag{35}$$

and that $\alpha<n^{-1}$ which is obtained from (35) for $i=1$. In particular, it follows by (35) that

$$\frac{\eta_1}{\eta_i}>\alpha n$$

for $i=2,\ldots,k$ which together with (33) implies that

$$n\tau+n\alpha(1-\tau)-1-\alpha n(k-1)-\alpha\geq 0$$

or equivalently

$$\tau\geq\frac{1+\alpha+\alpha n(k-2)}{n(1-\alpha)}\triangleq f(\alpha,n,k)\,.\tag{36}$$

Differentiating $f(\alpha,n,k)$ with respect to α yields

$$\frac{\partial}{\partial\alpha}f(\alpha,n,k)=\frac{n(k-2)+2}{n(1-\alpha)^2}$$

which implies that $f(\alpha,n,k)$ is increasing in α for $k\geq 2$ and therefore it follows that

$$\tau\geq\frac{1}{n}\tag{37}$$

which is obtained by letting $\alpha=0$ in (36). When $k=1$ it follows from (36) that

$$\tau\geq\frac{1+\alpha-\alpha n}{n(1-\alpha)}\tag{38}$$

The two cases in (37) and (38) will be handled separately starting with $k=1$ and (38).

To this end, assume that $k=1$ and note that $\mathbf{A}_1$ can be written, using (23) and (24), as

$$\begin{aligned}\mathbf{A}_1=&\sum_{i=1}^{n}\eta_i\mathbf{w}_i\mathbf{w}_i^{\mathrm{H}}\\=&\eta_2\left(\frac{\eta_1}{\eta_2}\mathbf{w}_1\mathbf{w}_1^{\mathrm{H}}+\sum_{i=2}^{n}\frac{\eta_i}{\eta_2}\mathbf{w}_i\mathbf{w}_i^{\mathrm{H}}\right)\\\succeq&\eta_2\left(\alpha\mathbf{w}_1\mathbf{w}_1^{\mathrm{H}}+\sum_{i=2}^{n}\mathbf{w}_i\mathbf{w}_i^{\mathrm{H}}\right)\end{aligned}\tag{39}$$

where

$$\frac{\eta_1}{\eta_2}=\alpha\quad\text{and}\quad\frac{\eta_i}{\eta_2}\geq 1\,,\ i=2,\ldots,n,$$

has been used in the last inequality. In the above, we have used $\succeq$ ($\preceq$) to denote the partial matrix ordering induced by the positive semi-definite cone, i.e., for Hermitian matrices $\mathbf{X},\mathbf{Y}\in\mathbb{C}^{r\times r}$ the notation $\mathbf{X}\succeq\mathbf{Y}$ ($\mathbf{Y}\preceq\mathbf{X}$) means that $\mathbf{X}-\mathbf{Y}$ is positive semi-definite. In particular, $\mathbf{X}\succeq\mathbf{Y}$ implies that $\lambda_i(\mathbf{X})\geq\lambda_i(\mathbf{Y})$ for $i=1,\ldots,r$. Defining

$$\mathbf{B}\triangleq\alpha\mathbf{w}_1\mathbf{w}_1^{\mathrm{H}}+\sum_{i=2}^{n}\mathbf{w}_i\mathbf{w}_i^{\mathrm{H}}\in\mathbb{C}^{(n-1)\times(n-1)}\,,$$

we obtain from (39) that $\mathbf{A}_1\succeq\eta_2\mathbf{B}$. Thus, $\lambda_1(\mathbf{A}_1)\geq\eta_2\lambda_1(\mathbf{B})$ and what remains to be shown is that $\lambda_1(\mathbf{B})\geq n^{-1}$. To this end, note that, since $\alpha<1$, it follows that

$$\mathbf{B}\preceq\sum_{i=1}^{n}\mathbf{w}_i\mathbf{w}_i^{\mathrm{H}}=\mathbf{I}$$

and, in particular, $\lambda_i(\mathbf{B})\leq 1$ for $i=1,\ldots,n-1$. At the same time,

$$\sum_{i=1}^{n-1}\lambda_i(\mathbf{B})=\mathrm{Tr}(\mathbf{B})=\alpha\|\mathbf{w}_1\|^2+\sum_{i=2}^{n}\|\mathbf{w}_i\|^2\,.\tag{40}$$

Since $|v_i|^2+\|\mathbf{w}_i\|^2=\|\mathbf{u}_i\|^2=1$ from (24), it follows from (31) that $\|\mathbf{w}_1\|^2=1-\tau$, since $k=1$, and

$$\sum_{i=2}^{n}\|\mathbf{w}_i\|^2=\sum_{i=2}^{n}(1-|v_i|^2)=n-2+\tau\,.$$

Combining this with (40) yields

$$\begin{aligned}\sum_{i=1}^{n-1}\lambda_i(\mathbf{B}) &= \alpha(1-\tau)+n-2+\tau \\ &\geq \frac{\alpha+n^2-2n+1}{n}=(n-2)+\frac{1+\alpha}{n}\end{aligned}$$

where (38) was used to establish the inequality. Equivalently,

$$\lambda_1(\mathbf{B}) \geq \frac{1+\alpha}{n}+(n-2)-\sum_{i=2}^{n-1}\lambda_i(\mathbf{B}) \,. \tag{41}$$

However, since $\lambda_i(\mathbf{B}) \leq 1$ for $i=2,\ldots,n-1$ this implies that

$$\lambda_1(\mathbf{B}) \geq \frac{1+\alpha}{n}+(n-2)-(n-2) \geq \frac{1}{n}$$

which proves that $\lambda_1(\mathbf{A}_1) \geq n^{-1}\lambda_2(\mathbf{A})$ since $\lambda_1(\mathbf{A}_1) \geq \eta_2\lambda_1(\mathbf{B})$ and $\eta_2 \triangleq \lambda_2(\mathbf{A})$.

When $k \geq 2$ it is sufficient to consider the lower bound on $\mathbf{A}_1$ given by

$$\mathbf{A}_1 \succeq \sum_{i=k+1}^{n}\eta_i\mathbf{w}_i\mathbf{w}_i^{\mathrm{H}} \succeq \eta_{k+1}\mathbf{C} \tag{42}$$

where

$$\mathbf{C} \triangleq \sum_{i=k+1}^{n}\mathbf{w}_i\mathbf{w}_i^{\mathrm{H}} \preceq \mathbf{I}\,. \tag{43}$$

Since the rank of $\mathbf{C}$ is at most $n-k$ it follows that

$$\begin{aligned}\sum_{i=k}^{n-1}\lambda_i(\mathbf{C}) &= \sum_{i=1}^{n-1}\lambda_i(\mathbf{C})=\mathrm{Tr}(\mathbf{C}) \\ &= \sum_{i=k+1}^{n}\|\mathbf{w}_i\|^2=n-k-1+\tau\end{aligned}$$

where $|v_i|^2+\|\mathbf{w}_i\|^2=1$ and (32) was used to establish the last equality. Similar to before,

$$\lambda_k(\mathbf{C}) \geq \tau+(n-k-1)-\sum_{i=k+1}^{n-1}\lambda_i(\mathbf{C}) \geq \frac{1}{n}$$

where $\lambda_i(\mathbf{C}) \leq 1$ and (37) was used. Using (42) yields

$$\lambda_k(\mathbf{A}_1) \geq \eta_{k+1}\lambda_k(\mathbf{C}) \geq n^{-1}\lambda_{k+1}(\mathbf{A})$$

since $\eta_{k+1} \triangleq \lambda_{k+1}(\mathbf{A})$. This concludes the proof. ∎

References

[1] J. Jaldén, L. G. Barbero, B. Ottersten, and J. S. Thompson, "Full diversity detection in MIMO systems with a fixed-complexity sphere decoder," in *Proc. IEEE International Conference on Acoustics, Speech, and Signal Processing, ICASSP*, vol. 3, Apr. 2007, pp. 49–52.

[2] I. Telatar, "Capacity of multi-antenna gaussian channels," *European Transantions on Telecommunication*, vol. 10, no. 6, pp. 585–596, Dec. 1999.

[3] D. Tse and P. Viswanath, *Fundamentals of Wireless Communication*. Cambridge University Press, 2005.

[4] L. G. Barbero and J. S. Thompson, "Fixing the complexity of the sphere decoder for MIMO detection," *IEEE Transactions on Wireless Communications*, vol. 7, no. 6, pp. 2131–2142, June 2008.

[5] ——, "Rapid prototyping of a fixed-throughput sphere decoder for MIMO systems," in *Proc. IEEE International Conference on Communications, ICC*, vol. 7, June 2006, pp. 3082–3087.

[6] ——, "FPGA design considerations in the implementation of a fixed-throughput sphere decoder for MIMO systems," in *Proc. The International Conference on Field-Programmable Logic, FPL*, Aug. 2006.

[7] A. D. Murugan, H. E. Gamal, M. O. Damen, and G. Caire, "A unified framework for tree search decoding: rediscovering the sequential decoder," *IEEE Transactions on Information Theory*, vol. 52, no. 3, pp. 933– 953, Mar. 2006.

[8] J. Jaldén and B. Ottersten, "On the complexity of sphere decoding in digital communications," *IEEE Transactions on Signal Processing*, vol. 53, no. 4, pp. 1474–1484, Apr. 2005.

[9] A. Burg, M. Borgmann, M. Wenk, M. Zellweger, W. Fichtner, and H. Bölcskei, "VLSI implementation of MIMO detection using the sphere decoding algorithm," *IEEE Journal of Solid-State Circuits*, vol. 40, no. 7, pp. 1566–1577, July 2005.

[10] M. O. Damen, H. E. Gamal, and G. Caire, "On maximum-likelihood detection and the search for the closest lattice point," *IEEE Transactions on Information Theory*, vol. 49, no. 10, pp. 2389–2401, Oct. 2003.

[11] H. Artés, D. Seethaler, and F. Hlawatsch, "Efficient detection algorithms for MIMO channels: a geometrical approach to approximate ML detection," *IEEE Transactions on Signal Processing*, vol. 51, no. 11, pp. 2808–2820, Nov. 2003.

[12] Z. Guo and P. Nilsson, "Algorithm and implementation of the K-best sphere decoding for MIMO detection," *IEEE Journal on Selected Areas in Communications*, vol. 24, no. 3, pp. 491–503, Mar. 2006.

[13] J. B. Anderson and S. Mohan, "Sequential coding algorithms: A survey and cost analysis," *IEEE Transactions on Communications*, vol. 32, no. 2, pp. 169–176, Feb. 1984.

[14] W. Zhao and G. B. Giannakis, "Reduced complexity closest point decoding algorithms for random lattices," *IEEE Transactions on Wireless Communications*, vol. 5, no. 1, pp. 101–111, Jan. 2006.

[15] C. Schnorr and M. Euchner, "Lattice basis reduction: improved practical algorithms and solving subset sum problems," *Mathematical Programming*, vol. 66, pp. 181–199, 1994.

[16] P. W. Wolniansky, G. J. Foschini, G. D. Golden, and R. A. Valenzuela, "V-BLAST: An architecture for realizing very high data rates over the rich-scattering wireless channel," in *Proc. URSI ISSSE '98*, Atlanta, GA, Sept. 1998, pp. 295–300.

[17] H. Zhu, Z. Lei, and F. P. S. Chin, "An improved square-root algorithm for BLAST," *IEEE Signal Processing Letters*, vol. 11, no. 9, pp. 772–775, Sept. 2004.

[18] W.-J. Choi, R. Negi, and J. M. Cioffi, "Combined ML and DFE decoding for the V-BLAST system," in *Proc. IEEE International Conference on Communications, ICC*, vol. 3, New Orleans, LA, June 2000, pp. 1243–1248.

[19] D. W. Walters and J. R. Barry, "The Chase family of detection algorithms for multiple-input multiple-output channels," in *Proc. IEEE Global Telecommunications Conference, GLOBECOM*, vol. 4, Dallas, TX, Dec. 2004, pp. 2635–2639.

[20] Y. Li and Z.-Q. Luo, "Parallel detection for V-BLAST system," in *Proc. IEEE International Conference on Communications, ICC*, vol. 1, New York, NY, Apr. 2002, pp. 340–344.

[21] Z. Lei, Y. Dai, and S. Sun, "A low complexity near ML V-BLAST algorithm," in *Proc. IEEE Vehicular Technology Conference, VTC*, vol. 2, Dallas, TX, Sept. 2005, pp. 942–946.

[22] C. Mun, "Transmit-antenna selection for spatial multiplexing with ordered successive interference cancellation," *IEEE Transactions on Communications*, vol. 54, no. 3, pp. 423–429, Mar. 2006.

[23] H. Zhang, H. Dai, Q. Zhou, and B. L. Hughes, "On the diversity order of spatial multiplexing systems with transmit antenna selection: A geometrical approach," *IEEE Transactions on Information Theory*, vol. 52, no. 12, pp. 5297–5311, Dec. 2006.

[24] R. W. Heath Jr., S. Sandhu, and A. Paulraj, "Antenna selection for spatial multiplexing systems with linear receivers," *IEEE Communications Letters*, vol. 5, no. 4, pp. 142–144, Apr. 2001.

[25] J. Jaldén and B. Ottersten, "On the maximal diversity order of spatial multiplexing with transmit antenna selection," *IEEE Transactions on Information Theory*, vol. 53, no. 11, pp. 4273–4276, Nov. 2007.

[26] M. Gharavi-Alkhansari and A. B. Gershman, "Fast antenna subset selection in mimo systems," *IEEE Transactions on Signal Processing*, vol. 52, no. 2, pp. 339–347, 2004.

[27] Y. Jiang, X. Zheng, and J. Li, "Asymptotic performance analysis of V-BLAST," *Proc. IEEE Global Telecommunications Conference, GLOBECOM*, vol. 6, pp. 3882–3886, 2005.

[28] R. A. Horn and C. R. Johnson, *Matrix Analysis*. Cambridge University Press, 1985.

[29] L. G. Ordóñez, D. P. Palomar, A. Pagès-Zamora, and J. R. Fonollosa, "High-SNR analytical performance of spatial multiplexing MIMO systems with CSI," *IEEE Transactions on Signal Processing*, vol. 55, no. 11, pp. 5447–5463, Nov. 2007.

[30] L. Zheng and D. N. C. Tse, "Diversity and multiplexing: A fundamental tradeoff in multiple-antenna channels," *IEEE Transactions on Information Theory*, vol. 49, no. 5, pp. 1073–1096, May 2003.

[31] N. Prasad and M. K. Varanasi, "Analysis of decision feedback detection for MIMO Rayleigh-fading channels and the optimization of power and rate allocations," *IEEE Transactions on Information Theory*, vol. 50, no. 6, pp. 1009–1025, June 2004.

[32] J. Jaldén and G. Matz, "MIMO receiver diversity in general fading," in *Proc. IEEE International Conference on Acoustics, Speech, and Signal Processing, ICASSP*, Apr. 2008, pp. 2837–2840.